
Plasma based XUV Sources for Metrology Applications

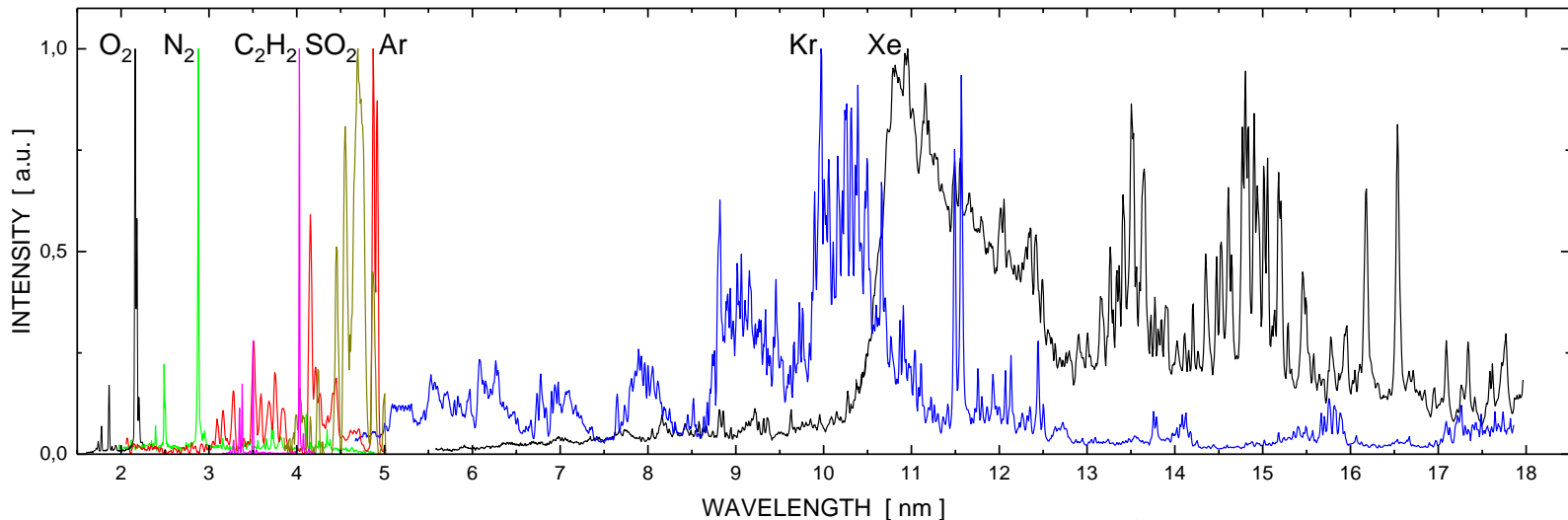
Klaus Bergmann, Jochen Vieker, Alexander von Wezyk
2017 EUV Source Workshop, 8.11.2017, Dublin

Current activities on XUV sources at ILT

Water window

Beyond EUV

13.5 nm



- single line for x-ray microscopy
- „broadband” emission for surface analysis tools

- technical solution for regenerative LPP targets
- identification of efficient emitter
- metrology sources

- sources for inspection
- optimization of brightness and power scaling at 13.5 nm
- increase of long term stability

This Paper !

S53_dublin2017.pptx

Consideration on 6.x nm emitter for LPP

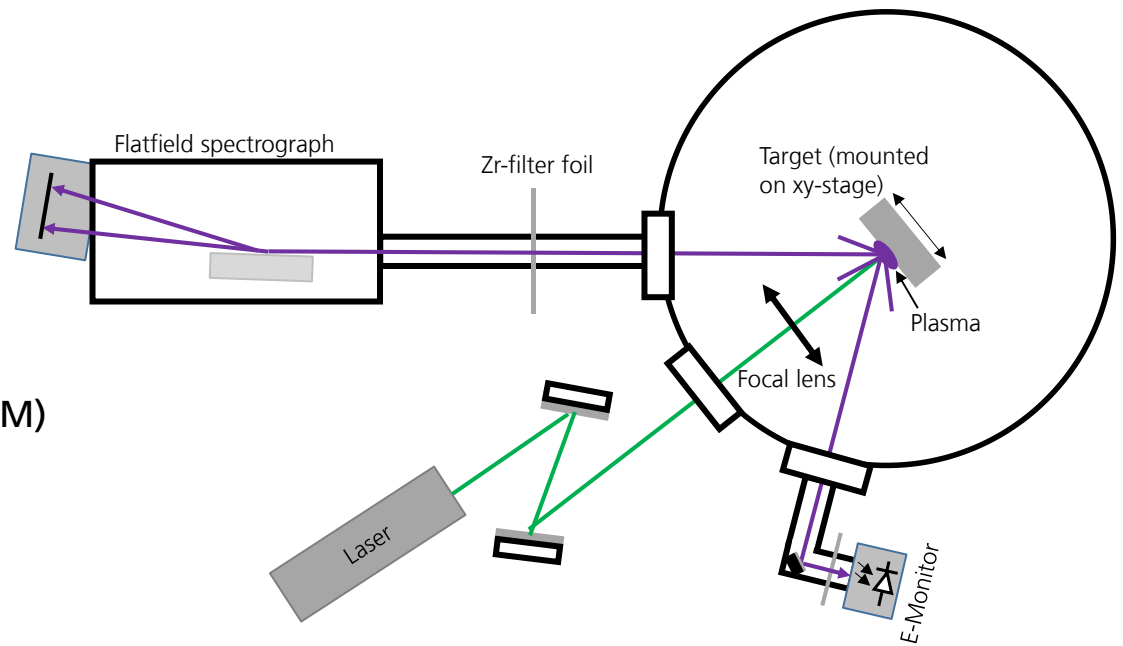
	Ionisation levels	Comments
Gd	~ XV – XXV	<ul style="list-style-type: none"> Known as efficient emitter due to UTA's around 6.x nm High melting point ($T_m > 1300^\circ\text{C}$) Not practical for liquid/regenerative targets
Tb	~ XIV – XXIV	
Al	~ VII – X	<ul style="list-style-type: none"> Lower melting point compared to Gd/Tb "Many" resonance lines within 5 – 8 nm Line emission better matched to small ML bandwidth
Mg	~ VIII – XI	
Xe	~ X	<ul style="list-style-type: none"> Gaseous emitter suited for DPP sources Broadband emission around 6.x nm Less efficient compared to Gd/Tb
Kr	~ IX	

Experimental Set-up: Comparison of 6.x nm emitter

Experiments in cooperation with
Rhein Ahr Campus (Remagen)

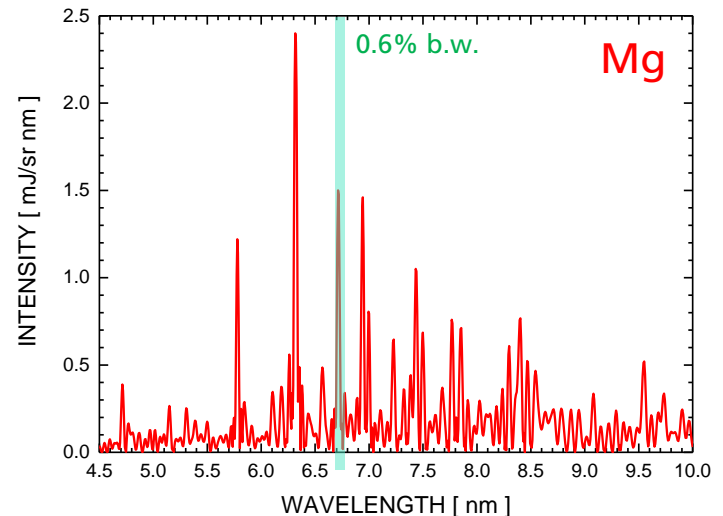
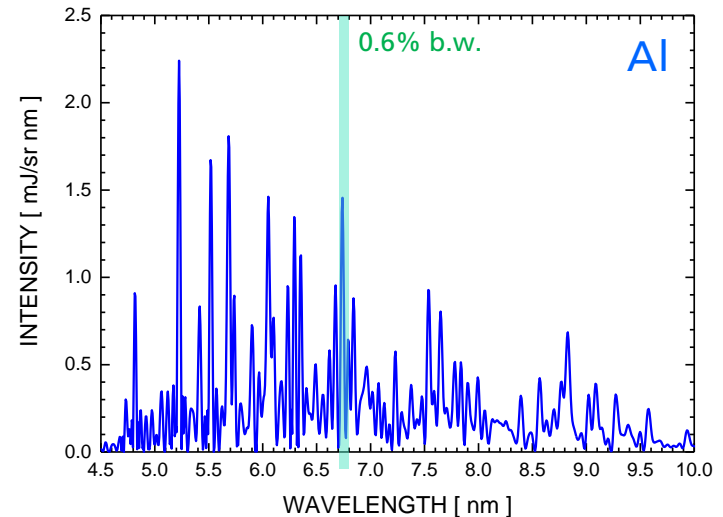
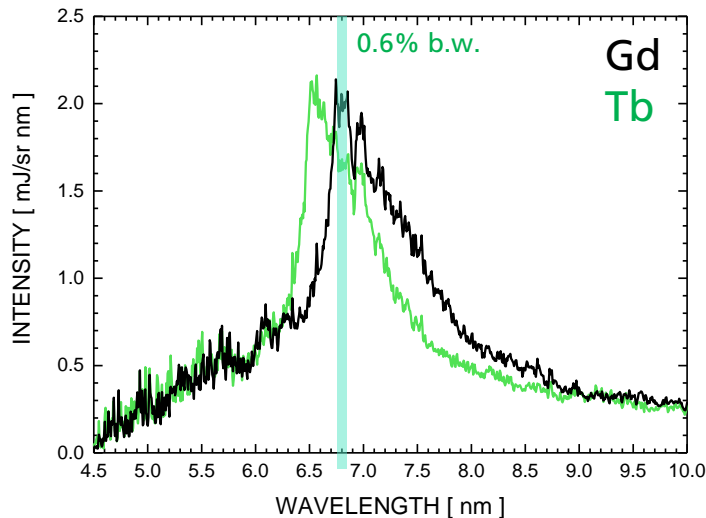
Coherent infinity laser:

- Wavelength: 532 nm
- Pulse energy: ~140 mJ
- Pulse length: 3 ns
- Rep.-rate: 10 Hz
- Typical focus size: 40 μm (FWHM)
- Typical intensity: $3 \times 10^{12} \text{ W/cm}^2$



Result 6.x nm: Alternative emitter for LPP

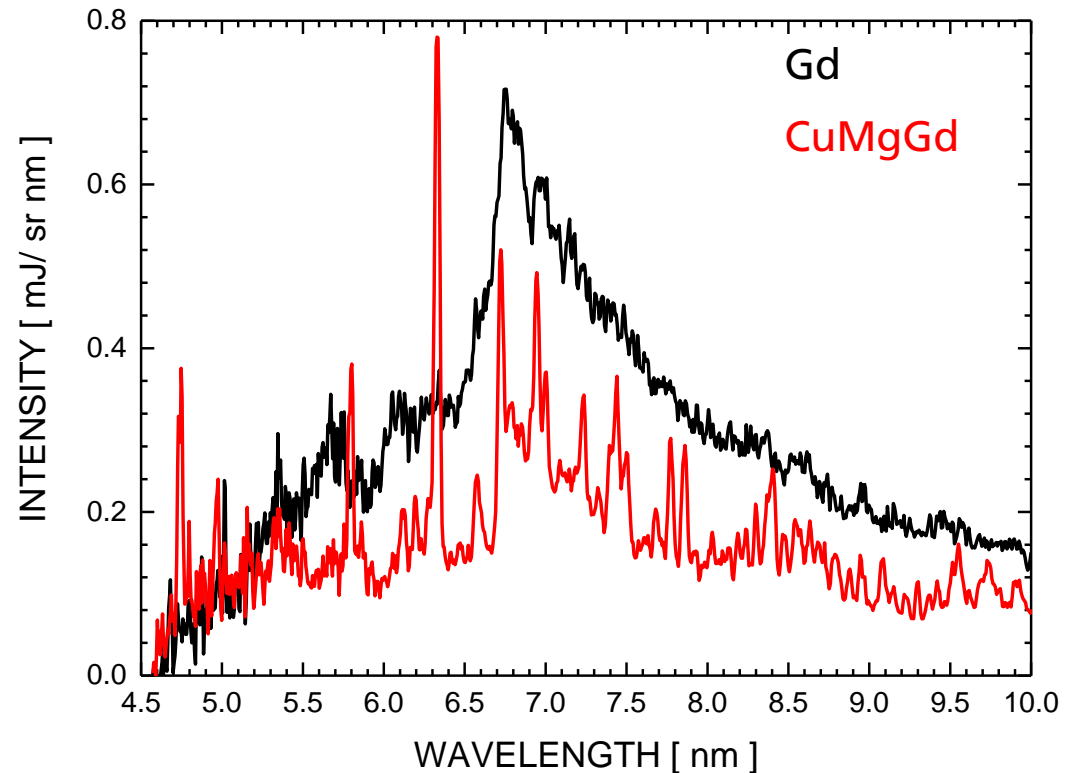
- Gd/Tb emission comparable to literature data for $\lambda_{\text{laser}} = 532 \text{ nm}$
CE $\sim 0,25\%/(2\pi\text{sr } 0.6 \% \text{ b.w.}) @ 6.7 \text{ nm}$
- similar peak brightness in lines for Al and Mg



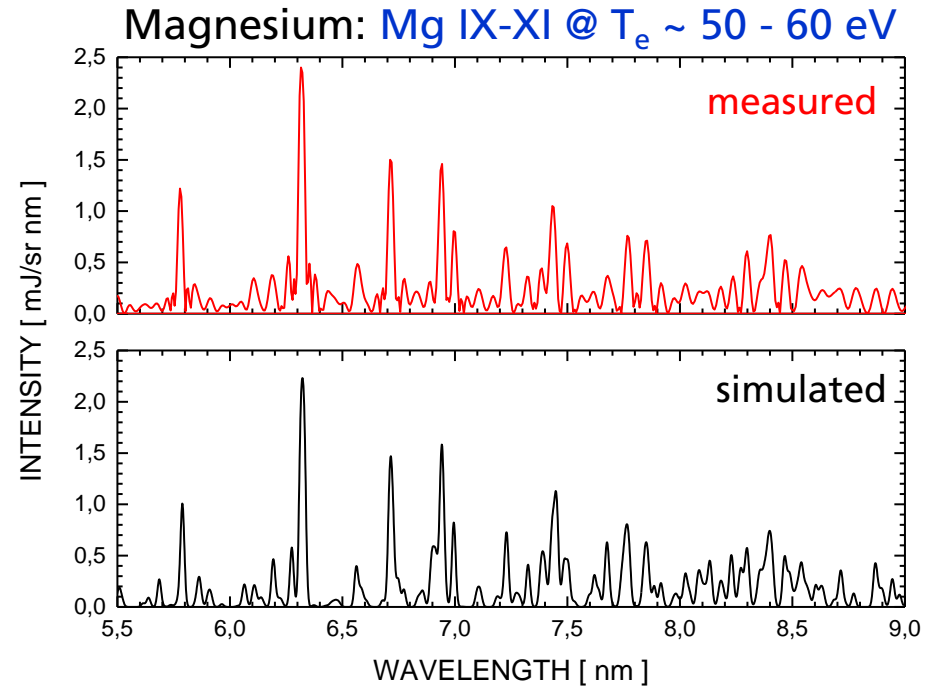
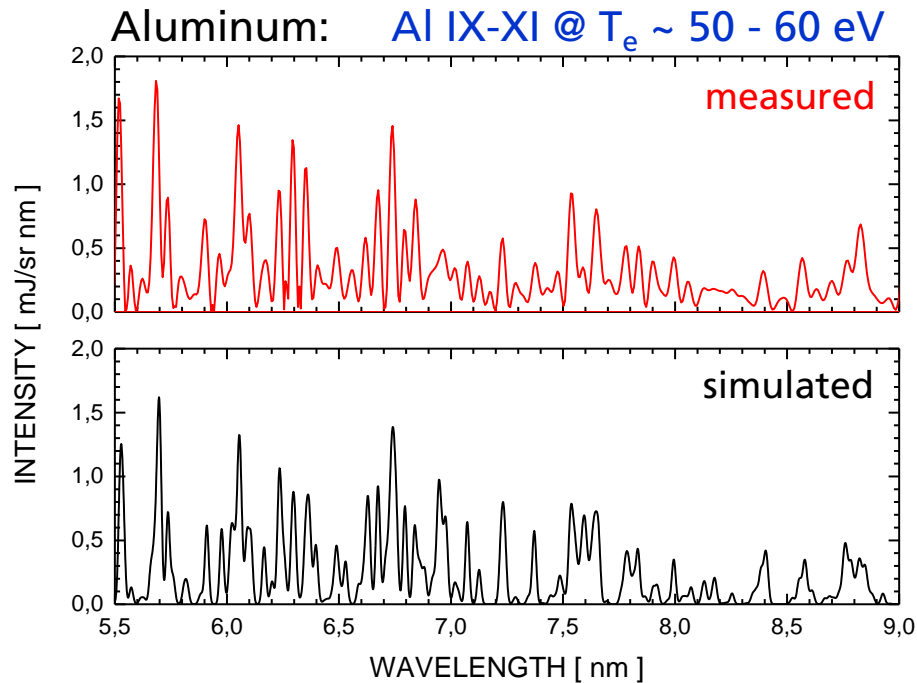
LPP emission spectra: Comparison Gd/CuMgGd

Melting point of CuMgGd :
< 500°C

- Same conditions for both targets
- Gd emission of alloy is reduced by factor 2
- Gd ion density in alloy is reduced by factor $\gg 2$ (2% atomic density)
- Behavior in agreement with theoretical considerations
- Strong line emission from Mg at 6.7 nm



Simulation of emission spectra (Al, Mg)



Spectral radiance :

$$L(\lambda) = \frac{j(\lambda)}{\chi(\lambda)} \cdot (1 - e^{-\chi(\lambda)d})$$

$$j(\lambda) = \sum_i j^i(\lambda) = \sum_i \frac{hc}{4\pi\lambda} A_{ul}^i n_u^i f^i(\lambda) \quad \begin{array}{l} u: \text{upper level} \\ l: \text{lower level} \end{array}$$

$$\chi(\lambda) = \sum_i \chi^i(\lambda) = \sum_i \frac{h\lambda}{c} (B_{lu}^i n_l^i - B_{ul}^i n_u^i) f^i(\lambda)$$

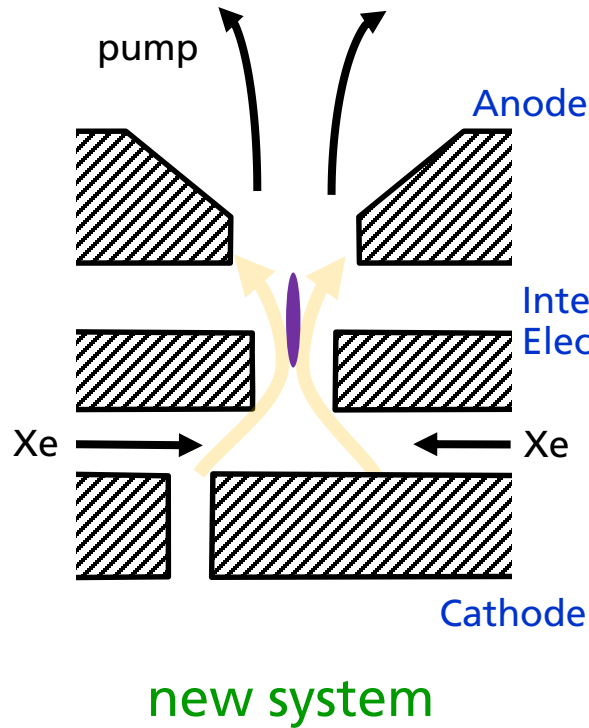
Discharge based XUV Source: 13.5 nm inband emission



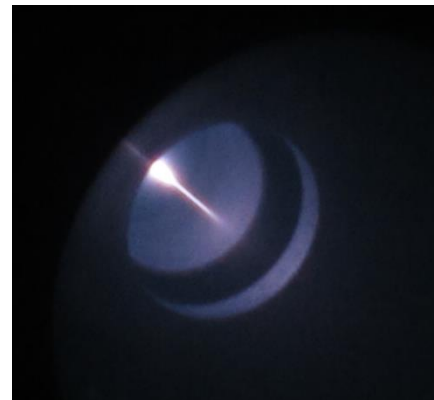
Xenon based FS5440 (13.5 nm, 2 % b.w.)

- Inband Power: $> 40 \text{ W}/2\pi\text{sr}$
- EUV pulse energy: $> 4 \text{ mJ/sr}$
- Typ. repetition rate: 1500 Hz
- Avg. peak brightness: $12 \text{ W/mm}^2\text{sr}$

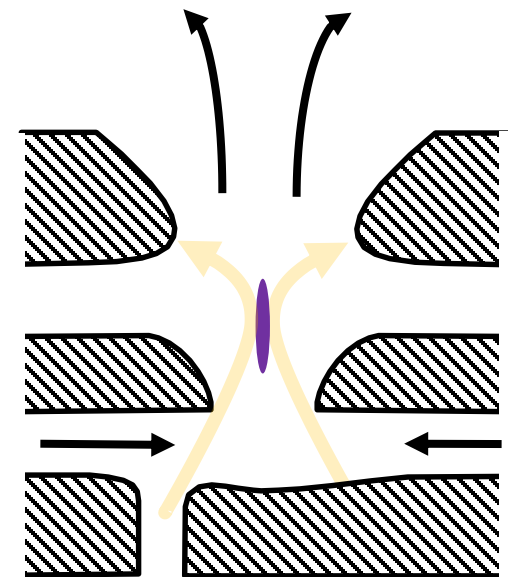
Discharge based XUV Source: Electrode geometry



- EUV generation between IP and Anode
- erosion pattern will influence EUV generation
- better understanding of relevant parameters to keep CE constant (e.g., gas flow, initial geometry)

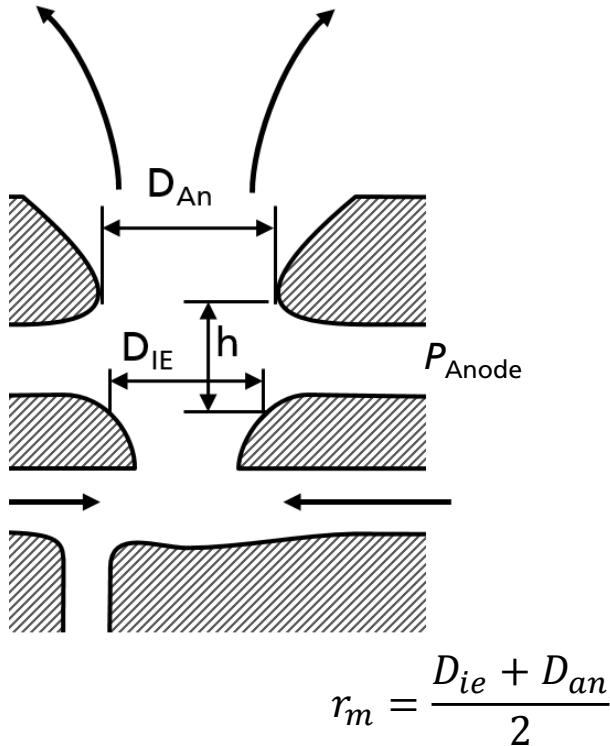


Side view on plasma (visible)



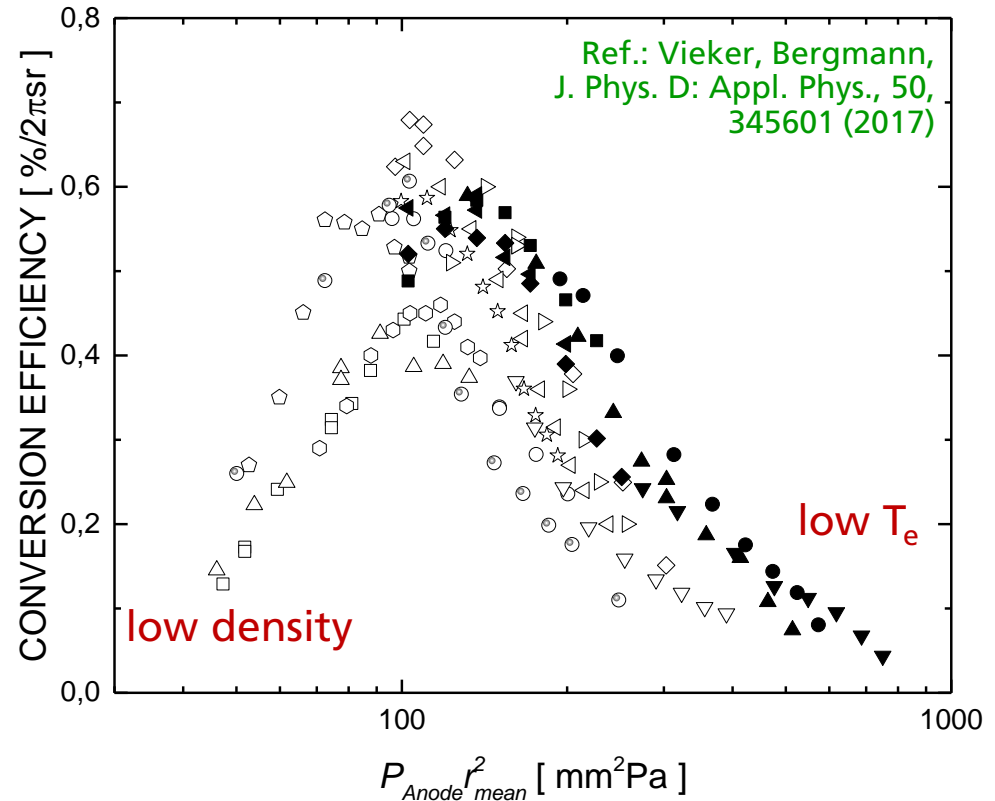
after operation

CE dependency on electrode shape



“average line density”

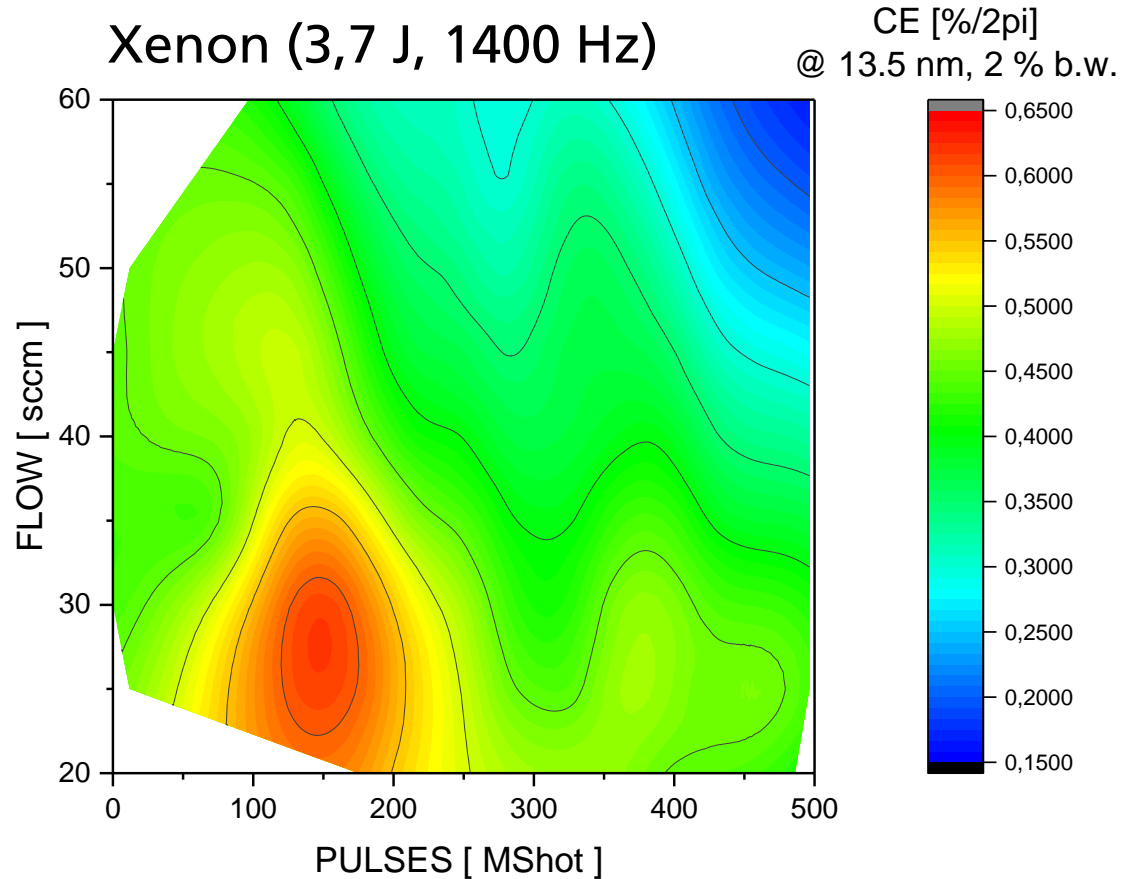
$$P_{Anode} r_m^2$$



- similar CE for same “average line density”
- different values for $P_{Anode} r_m^2$ due to erosion and variation of initial diameters

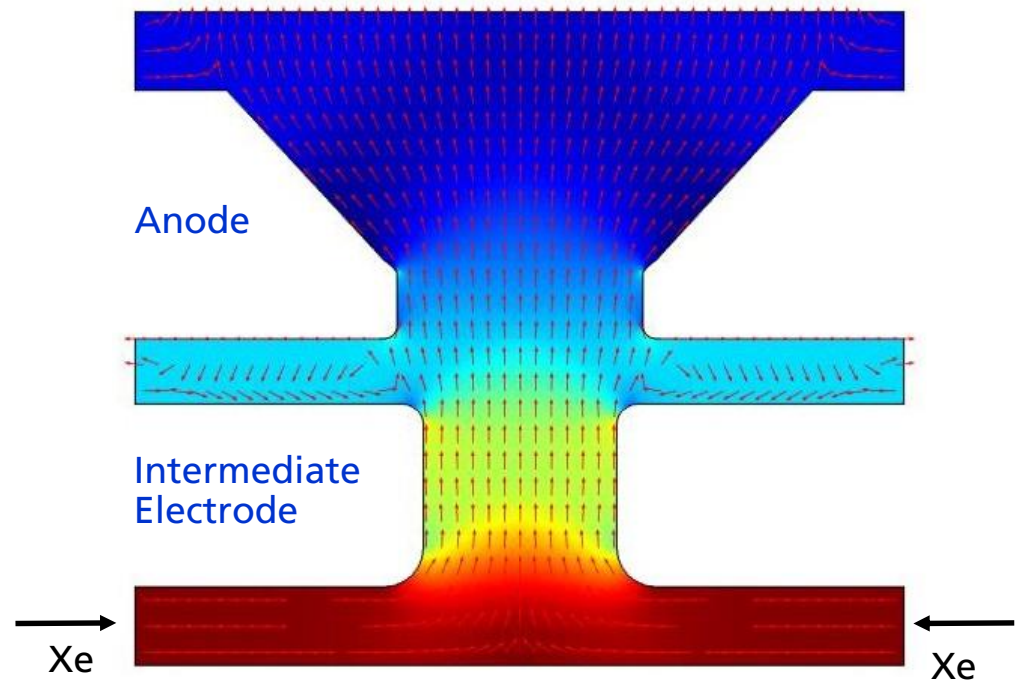
Long term behavior of conversion efficiency

- deformation of electrodes influences accessible $P_{\text{Anode}} r_m^2$
- change of CE dependence with shots in agreement with observed $P_{\text{Anode}} r_m^2$ behavior
- access of optimum $P_{\text{Anode}} r_m^2$ after 100 Mio pulses



Simulation of neutral gas density distribution

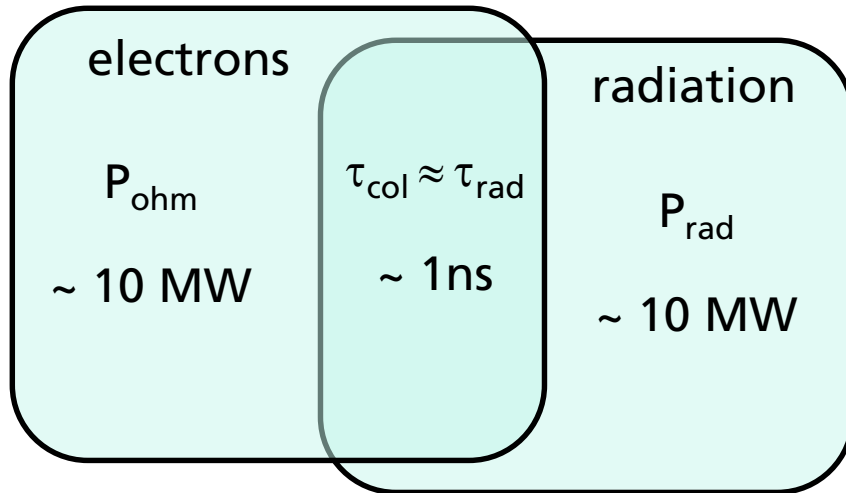
- more accurate estimation of density distribution based on flow simulations
- good agreement with measured pressures at cathode and anode
- prediction of electrode shapes (erosion, initial shape) on density distribution



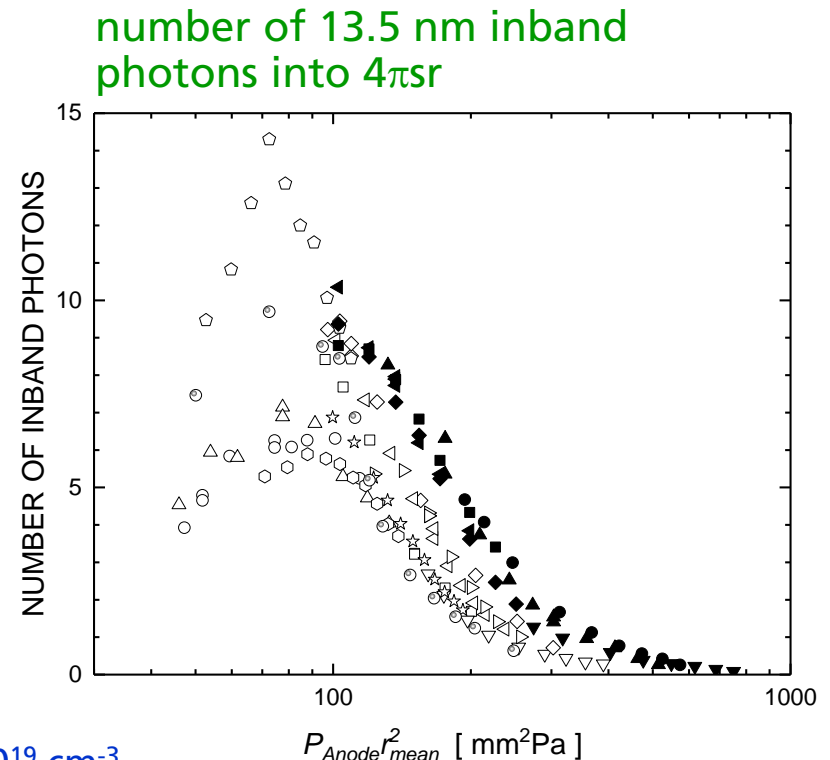
Remarks on the excitation of EUV photons...(1)

- ~100 EUV emission processes per ion
- balance of Ohmic Heating and Radiation
- state of high energy conversion
(several %/ $2\pi sr$ inband at 13.5 nm)

Energy Conversion
(rough estimation)

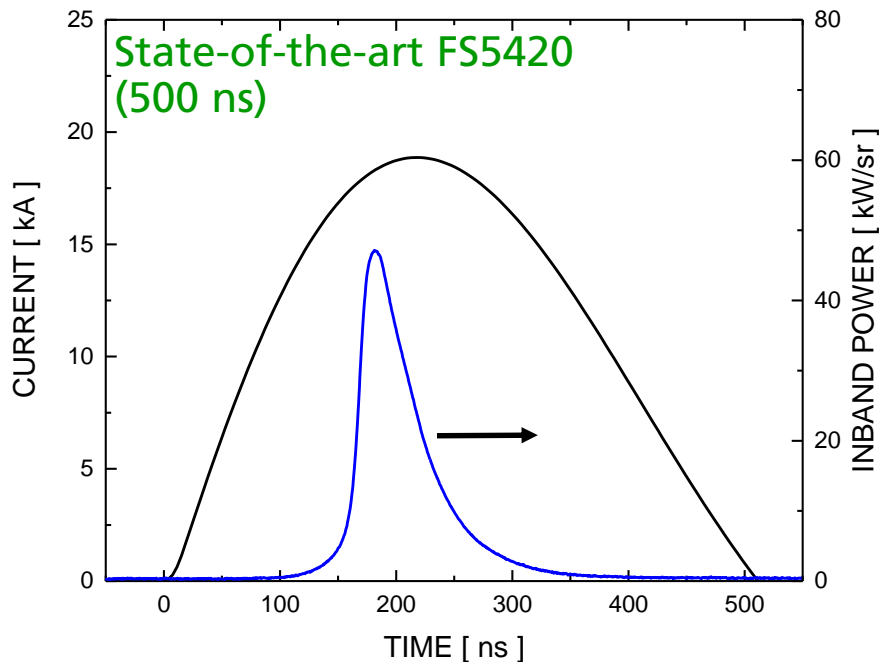


$n_e \sim 10^{19} \text{ cm}^{-3}$
 $T_e \sim 50 \text{ eV}$
 $N_{emit} \sim 4 \cdot 10^{14}$
 $r_{pl} \sim 200 \text{ } \mu\text{m}$
 $I \sim 10 \text{ kA}$

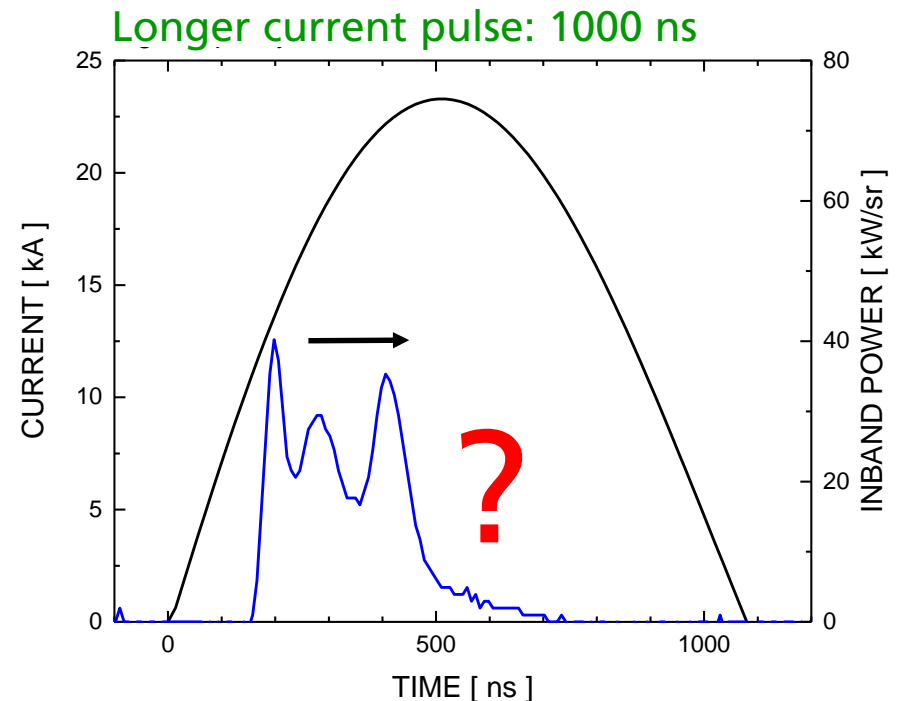


Ref.: Vieker, Bergmann,
J. Phys. D: Appl. Phys., 50,
345601 (2017)

Remarks on the excitation of EUV photons...(2)



- longer EUV emission with increase of pulse duration
- decrease of EUV emission after current maximum – Reason ??
- optimization potential, if EUV emission could be prolonged



Summary

- Emission spectra of Al, Mg as alternative emitters around 6.x nm (small bandwidth)
- Proposal of Gd/Tb based alloys for 6.x nm target material (GdCuMg with $T_m < 500^\circ\text{C}$)
- Quantification of the correlation between electrode shape and 13.5 nm inband CE for Xenon based discharge source
- Knowledge is base for solutions to extend the maintenance interval
- Identification of further optimization potential for the CE based on more efficient use of discharge current

See also Talk/Poster:

- (S74) Laboratory Tomographic Microscopy with Compact Plasma based Extreme Ultraviolet and soft x-ray Sources, Daniel Vicario
- (S76) Spectroscopic EUV reflectometry for characterization of thin films systems and determination of optical constants, Larissa Juschn